doi:10.1038/nature11002

# Patterning by controlled cracking

Koo Hyun Nam[1], Il H. Park[1] & Seung Hwan Ko[2]

**Crack formation drives material failure and is often regarded as a process to be avoided[1–3]. However, closer examination of cracking phenomena has revealed exquisitely intricate patterns such as spirals[4], oscillating[5,6,7] and branched[7] fracture paths and fractal geometries[8]. Here we demonstrate the controlled initiation, propagation and termination of a variety of channelled crack patterns in a film/substrate system[9–11] comprising a silicon nitride thin film deposited on a silicon substrate using low-pressure chemical vapour deposition. Micro-notches etched into the silicon substrate concentrated stress for crack initiation, which occurred spontaneously during deposition of the silicon nitride layer. We reproducibly created three distinct crack morphologies—straight, oscillatory and orderly bifurcated (stitchlike)—through careful selection of processing conditions and parameters. We induced direction changes by changing the system parameters, and we terminated propagation at pre-formed multi-step crack stops. We believe that our patterning technique presents new opportunities in nanofabrication and offers a starting point for atomic-scale pattern formation[12], which would be difficult even with current state-of-the-art nanofabrication methodologies.**

We have found that the tools and techniques for thin brittle material deposition drawn from conventional microfabrication technologies allow us to attain nearly ideal conditions for crack formation[13,14]. Low-pressure chemical vapour deposition of silicon nitride ($Si_3N_4$) thin films offers high levels of uniformity, reproducibility on planar surfaces and superior controllability for batch processing. A well refined, single-crystalline silicon substrate gives predictable thermal responses. Finally, standard silicon wafer and microfabrication techniques enable the control of processing conditions and facilitate post-fabrication processes. To control crack initiation at the desired position and orientation at microscopic scales, we used silicon etching to create 'micro-notch' structures which concentrate stress to initiate cracks. With uniform deposition of a cracking layer on the substrate, this technique can reduce undesirable effects, and permit the generation of cracks that are much more complex and controllable than those generated on as-fabricated samples. In the present case, the crack occurs on the thin $Si_3N_4$ layer during deposition, as a result of the film stress arising between that layer and the underlying material. Figure 1a shows the controlled formation of oscillating cracks on a $Si_3N_4$ thin film deposited on a silicon substrate with patterned notches. The geometric characteristics of the cracks, such as their wavelength and amplitude of oscillation, are influenced by the adjacent stress field, which is defined by the value of the film stress at the time of cracking. Thus, successful crack initiation can be achieved with a micro-notch designed with an optimal notch tip angle to concentrate stress (Supplementary Fig. 3). The characteristics of the notch determine the timing of crack initiation and, in turn, the condition of the substrate and cracking material where the propagation occurs. Thus, the design of a micro-notch changes the characteristics of the resulting cracks. We were able to achieve highly controllable crack initiation with 100% yield (Fig. 1a) through successful micro-notch design.

Because the orientations and shapes of cracks in the thin layer atop the silicon substrate are determined by the film stress occurring between two different materials, variations in the types and thicknesses of testing materials were thought to be significant factors that could alter the cracking response. Oscillating and straight cracks (Fig. 1b, c; left and middle images) are generated on a $Si_3N_4$ thin film deposited on silicon wafers of different crystallographic orientations (Supplementary Fig. 4) under controlled conditions. Both of those types of crack can coexist on a (100) silicon wafer, and in that case, they meet each other perpendicularly, as shown in Fig. 1d. Crack widths observed in this study varied between about 10 and 120 nm, with straight cracks generally narrower than oscillating cracks. Straight cracks are also observed when a silicon dioxide ($SiO_2$) film is deposited as an interlayer between the $Si_3N_4$ and the silicon substrate. In this circumstance, 'stitchlike' cracks, with non-propagating branches[3], can also form (Fig. 1b, c; right images). The non-propagating branches are caused by fluctuations in the available elastic energy, above and below the value required for branching. Unlike the straight cracks, the stitchlike cracks form adjacent to a pre-existing underlying crack in the $SiO_2$ interlayer. The highly ordered branching observed in the stitchlike cracks is unusual, and testifies to the very precisely controlled conditions of our study; crack bifurcation occurs at high energies, where instability is also more readily introduced[3,15]. The precise control of crack formation by micro-notching can yield predefined complex nano-patterning, as shown in Fig. 1e and Supplementary Fig. 5.

The three main types of crack can be created by controlling the processing conditions and system parameters, and by using the intrinsic crystallographic properties of the silicon substrate. Oscillating cracks are quite constant in profile along their length, and have a strong tendency to propagate in the $<110>$ direction through a (100) silicon wafer (Fig. 2a). Our oscillating cracks resemble those reported in refs 7 and 16, but are easier to create and can be reliably replicated. They should also be distinguished from previously studied 'through-the-thickness' cracks[3–8,14–16], which have frequently been used to study crack dynamics. In the present case, we have a two-dimensional, channelling crack that propagates towards, and through, the interface between two different materials, which is additionally characterized by an in-plane propagation across each of the materials[9–11] (Fig. 2b; and see Supplementary Information for further discussion of the physics of the oriented cracking).

When a crack's depth of penetration in the film/substrate system is shallow, it may propagate in several specific directions, owing to the different stress distributions in the film and the substrate[17]. For example, a straight crack shows several propagation directions in the vicinity of the $<100>$ orientation. However, when the crack's depth of penetration into the silicon wafer is increased, the crack propagation direction is more strongly influenced by the crystalline orientation of the substrate than by the anisotropically oriented stress distribution in the film/substrate system. We have found that if a propagating crack experiences a substantial change in either of these conditions, its propagation direction changes, in a manner resembling the refraction of light. As shown in Fig. 3, a change in the underlying material initially causes kinking[18,19] of the crack when it passes across the interface between the two different regions, and then maintenance of the new propagation direction. In the 'interlayer region', formed of a three-layer

[1]Research Center of MEMS Space Telescope, Department of Physics, Ewha Womans University, Daehyun-dong 11-1, Seodaemun-gu, Seoul 120-750, South Korea. [2]Applied Nano Technology and Science Lab, Department of Mechanical Engineering, Korea Advanced Institute of Science and Technology, 335 Daehak-ro, Yusong-Gu, Daejeon 305-701, South Korea.

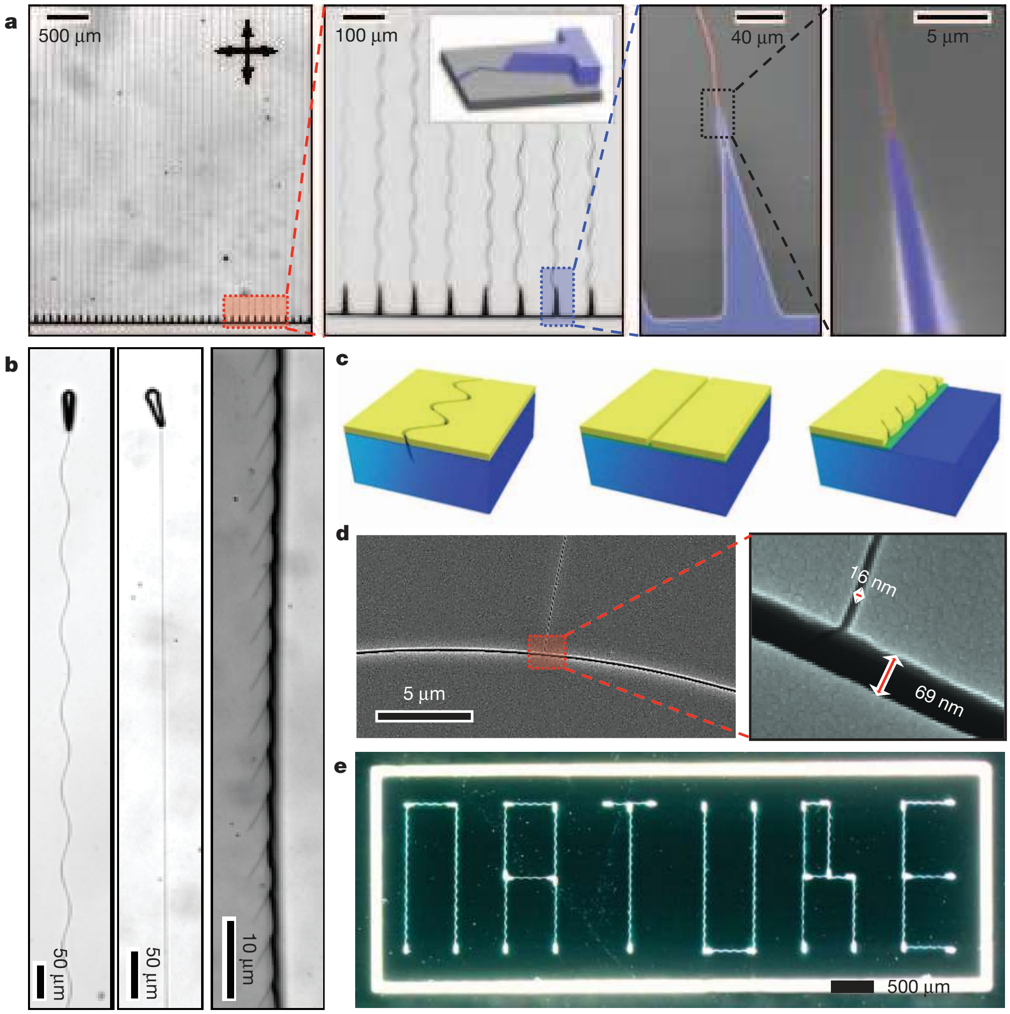


**Figure 1 | Crack control. a**, Optical and electron micrographs of oscillating crack initiation from micro-notches in a $Si_3N_4$ thin film deposited on (100) silicon. **b**, Left to right: an oscillating crack initiated from a micro-notch; a straight crack initiated from a micro-notch; and a stitchlike crack showing orderly bifurcated cracking with non-propagating branches. **c**, Schematic diagrams of each type of crack. Yellow, $Si_3N_4$ thin film; cyan, $SiO_2$ interlayer; blue, silicon wafer. **d**, Electron micrographs of cracks of different types and widths. The straight crack propagating vertically in the figure has much a smaller width than the oscillating crack running horizontally. **e**, Precise manipulation of oscillating cracks with crack notches to write the word 'NATURE'.

composite, or trimaterial[20,21], a $SiO_2$ interlayer acts as a buffer layer, suppressing the penetration of the crack into the silicon substrate. In the 'no-interlayer region', where the $SiO_2$ interlayer has been selectively etched away, the crack penetrates deeply into the substrate. (See Supplementary Information for further discussion of the crack refraction mechanism.) The cracks require an adequate distance of travel through these transition regions to establish the new mode of crack propagation. If the crack propagation distance is short, crack kinking is observed but not a stable straight or oscillatory mode (Fig. 3b).

Arresting crack propagation is important for the prevention of material failure, and the tailoring of controlled cracks can find use in engineered structures. As has been detailed in previous studies[22–25], several methods for limiting cracks have been developed, both through the addition of reinforcing materials and through the inclusion of

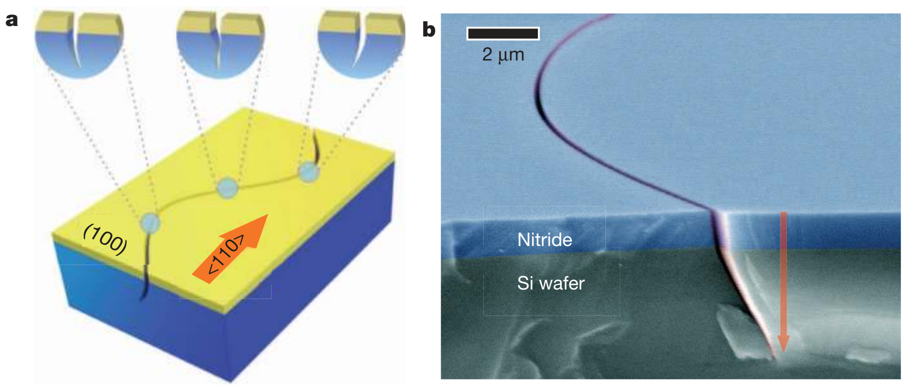


**Figure 2 | Formation mechanism of an oscillating crack. a**, Schematic figure of cracking materials and crack propagation, showing crystallographic orientations of the silicon substrate. Oscillating cracks tend to propagate in the <110> direction, and also penetrate downwards into the silicon substrate. These in-substrate cracks point towards the centre of the crack trajectory, displaying maximal angles from the vertical along the substrate's lowest energy cleavage plane, {111}, at the points farthest from the oscillating centre (as shown in the cross-sections above the plane). The penetration depth of the crack into the substrate depends, in part, on the substrate's bimaterial bending force, and, in turn, determines the amplitude of oscillation. (See Supplementary Information for further discussion.) **b**, Electron micrograph showing penetration of a crack into the silicon substrate (red arrow), angling towards the propagating centre of oscillation.

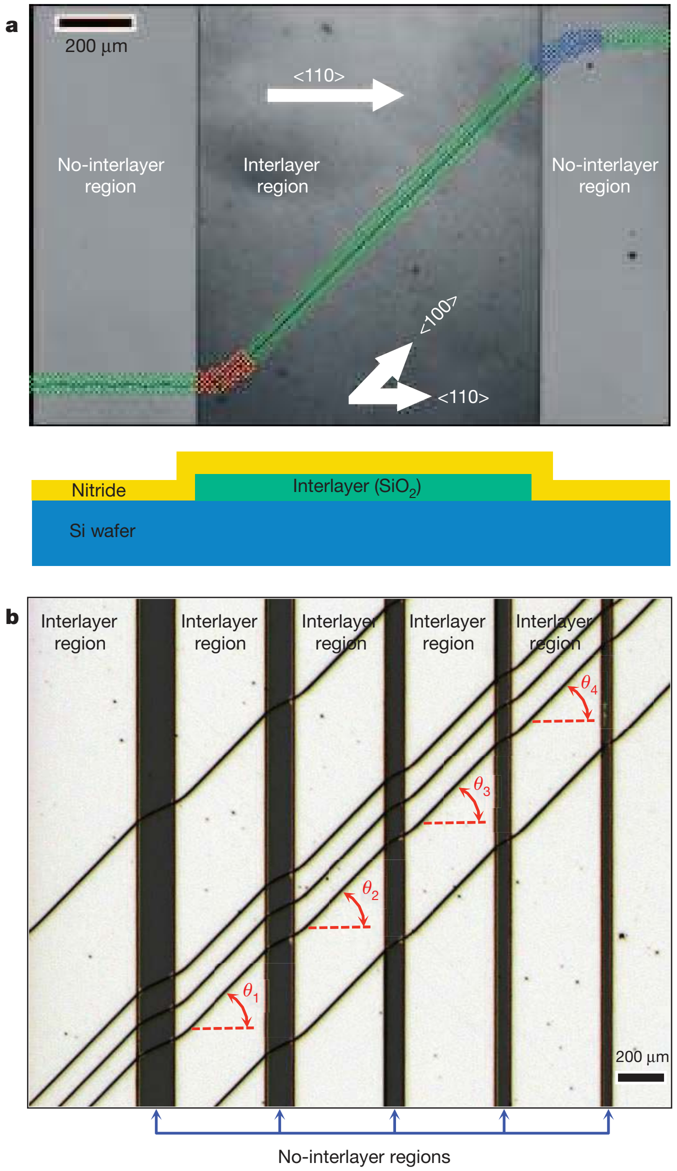


**Figure 3 | Crack refraction. a**, Cracks running through a $Si_3N_4$ film on a $SiO_2$ interlayer tend to propagate straight in the <100> direction, whereas oscillating cracks run in the <110> direction. (See also Supplementary Fig. 4.) When a crack passes across the interface between two different underlying configurations (shown in the schematic cross-section below), the crack trajectory kinks[18,19], until it attains the propagation direction appropriate to the configuration of the region through which it is then travelling. Two such 'transition regions' are highlighted in red and blue. **b**, Crack propagation across multiple alternating regions in which the no-interlayer regions are insufficiently wide to allow a full oscillation cycle to occur. Straight cracks in the interlayer regions, however, have sufficient distance to recover identical propagation angles ($\theta_1 = \theta_2 = \theta_3 = \theta_4$).

impurities to increase fracture resistance when a physical separation of the cracking materials is not possible. However, these methods introduce a material preparation step into the crack prevention process, and they are unable to precisely place crack stops at specific locations. In a film/substrate composite, varying the local stress in the film by altering the substrate geometry could, to an extent, affect the dynamics of cracks. However, in our cases the film continuity is barely affected by the structural geometry of the underlying materials, including the silicon substrate, because the $Si_3N_4$ thin film prepared by chemical vapour deposition is highly conformal. Because the stress field between the substrate and deposited film in this case is uniform, a crack will not stop propagating until it has reached the edge of the wafer.

If the stress drops during the propagation of a crack, the crack registers the disturbance of the driving force. When the driving force decreases to a value comparable to the crack resistance, the crack stops propagating. We attempted to decrease the driving force by fabricating a stair-profiled structure on the substrate. Fig. 4a, b shows a substrate patterned with terraced edges by deep reactive-ion etching; in these regions, the film stress drops sharply in front of the propagating crack. However, when overstress is present in the film, the surplus energy that remains after the consumption of the elastic energy is stored by the enhanced acceleration of a crack or extension of the substrate penetration. This excess energy is the major obstacle in the effort to terminate crack propagation. We have found that a significant change in the stress field to stop crack propagation is difficult in normal one-step structures fabricated by conventional etching processes (Fig. 4a). In this case, the crack recovers its driving force from the stored energy, which is then regenerated during the subsequent propagation. On the other hand (Fig. 4b), crack propagation terminates when multi-step structures are introduced to reduce the propagation distance to a level inadequate for the recovery of surplus energy within the travel region, at which point the stored energy becomes insufficient for further propagation of the crack. As shown in the left inset of Fig. 4b, we fabricated a stair profile with multiple steps of 5 μm height and width, and found that this structure is able to stop crack propagation with no failures (Fig. 4b, d), whereas a crack stop with a single step profile fails to terminate crack propagation (Fig. 4a, c). As such a stair structure is difficult to construct using conventional microfabrication processes, we invented a special single-step lithography method to fabricate stair-profile microstructures by intentional diffraction (see Supplementary Fig. 2 for process details). In addition to providing stress control, stair-profile microstructures are also able to disrupt the stress field by increasing the roughness of the etched surface, which in turn obstructs crack propagation. Another important feature of the crack stop is its ability to protect sampling regions from the intrusion of highly uncontrollable external cracks, which develop readily during the wafer dicing process (Fig. 4d). (See Supplementary Information for further discussion of the crack stoppage mechanism.) An isolated region enclosed and protected by a crack stop remains crack-free even after wafer dicing.

The precise control of crack initiation and termination by the proposed crack notches and stops may enable the development of a new, very simple approach for high-resolution, arbitrary nano-patterning of large-area substrates, as a potential alternative to such state-of-the-art approaches as electron-beam or high-energy beam lithography[26,27]. Large-area, high-resolution nano-patterning is challenging even with conventional electron-beam lithography, which is a very expensive, time-consuming and slow serial process[26,27]. By contrast, our approach is not limited by wafer size and can be easily scaled up to much larger wafer sizes with no increase in processing time and cost, owing to the parallel and self-generated process used in production. Furthermore, since the materials and fabrication processes used in this study are fully compatible with well developed, silicon-based integrated circuit processes, this technique should be readily applicable in the semiconductor industry, where the level of scale-down determines competitiveness. (See Supplementary Information for further discussion.)

So far, we have focused on an optimum combination of materials ($Si_3N_4$ thin films on silicon wafers) for the study of controlled cracking. Other material combinations might satisfy the criteria for triggering crystallographically oriented channelling cracks (see Supplementary Information). We expect that more precise control of dimensions, including crack width and depth, will be achieved through post-processing, such as additional conformal deposition[28] and polishing. Finally, more elaborate control of the experimental environment than has yet been achieved will open up new scientific insights and technological consequences of this phenomenon[1,2,13,14,29,30]. (See Supplementary Fig. 11 for more advanced crack manipulation possibilities.)

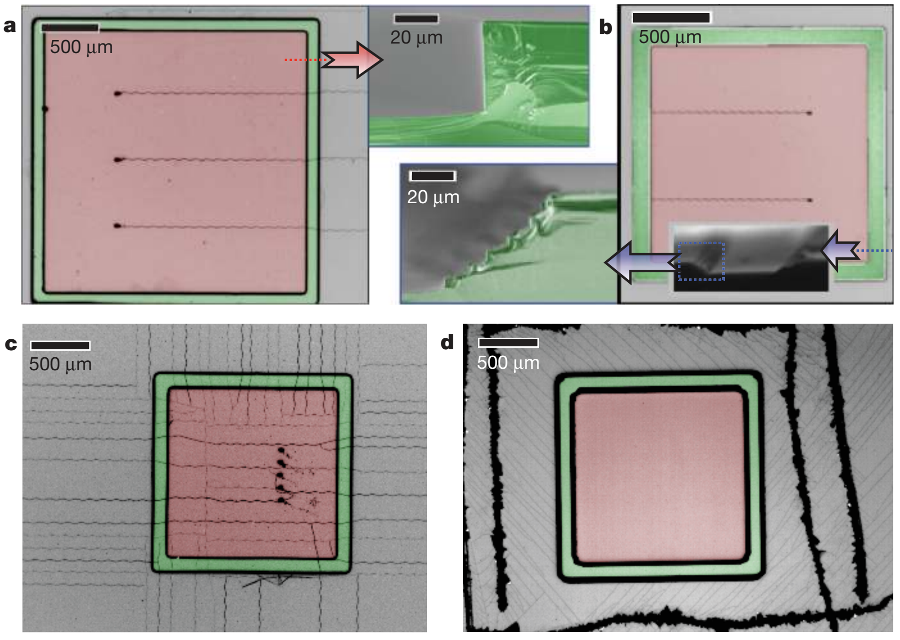


**Figure 4 | Crack termination. a**, Unsuccessful crack arrest. A box structure (green colour) intended for crack arrest is built using a one-step structure generated by conventional lithography. On the conformably deposited cracking layer, all cracks pass through the one-step structure (shown in cross-section in the electron micrograph at right) without stopping. **b**, Successful crack arrest. The same box structure, but with a multi-step edge fabricated by our new technique of diffraction-induced stairing lithography (DISL; Supplementary Fig. 2). In this case, all cracks terminate when they encounter the box structure (shown in cross-section in the electron micrograph at left). **c**, **d**, Additional examples of crack stoppage failure (**c**) and success (**d**). Structures etched in the silicon substrate without DISL influence the propagation of cracks to some extent, but are unable to cause termination.

## METHODS SUMMARY

Samples used in this study were made mostly from 525-µm-thick (100) silicon wafers, with (110) and (111) silicon samples used to observe the dependence of crack propagation on crystallographic orientation in silicon substrates. $Si_3N_4$ (stoichiometric silicon nitride) films were formed by thin-film deposition from a chemical precursor gas in a low-pressure environment at accurately controlled temperature (800 °C) and pressure (200 mtorr). Source gases and their mass flow rates were as follows: dichlorosilane ($H_2SiCl_2$) at 30 $cm^3$ STP $min^{-1}$ and ammonia ($NH_3$) at 100 $cm^3$ STP $min^{-1}$. $SiO_2$ interlayers were deposited at 1,000 °C by thermal oxidation, and we attempted various deposition thicknesses between 100 nm and 2 µm. The fabrication method for the crack initiation notch was designed to be an easy process involving few steps, and consequently variations in the structure of the notches were minimized. Although the height of a notch is determined by other structures fabricated together with the notch, the possibility of crack initiation at the notch reaches a satisfactory level when the height is more than 5 µm. For crack refraction, a $SiO_2$ interlayer was defined by chemical etching, and $Si_3N_4$ was deposited on the interlayer using the chemical thin film deposition procedure mentioned earlier. For details of the microfabrication process, see Supplementary Information.

**Received 21 November 2011; accepted 28 February 2012.**


1. Hellemans, A. Cracks: more than just a clean break. *Science* **281,** 943–944 (1998).
2. Livne, A., Bouchbinder, E., Svetlizky, I. & Fineberg, J. The near-tip fields of fast cracks. *Science* **327,** 1359–1363 (2010).
3. Broek, D. *Elementary Engineering Fracture Mechanics* 4th edn (Martinus Nijhoff Publishers, 1986).
4. Leung, K.-T., Jozsa, L., Ravasz, M. & Neda, Z. Pattern formation: spiral cracks without twisting. *Nature* **410,** 166 (2001).
5. Deegan, R. D., Petersan, P. J., Marder, M. & Swinney, H. L. Oscillating fracture paths in rubber. *Phys. Rev. Lett.* **88,** 014304 (2001).
6. Deegan, R. D. *et al.* Wavy and rough cracks in silicon. *Phys. Rev. E* **67,** 066209 (2003).
7. Yuse, A. & Sano, M. Transition between crack patterns in quenched glass plates. *Nature* **362,** 329–331 (1993).
8. Skjeltorp, A. T. & Meakin, P. Fracture in microsphere monolayers studied by experiment and computer simulation. *Nature* **335,** 424–426 (1988).
9. Hutchinson, J. W. & Suo, Z. Mixed mode cracking in layered materials. *Adv. Appl. Mech.* **29,** 63–191 (1991).
10. Beuth, J. L. Jr. Cracking of thin bonded films in residual tension. *Int. J. Solids Struct.* **29,** 1657–1675 (1992).
11. Ye, T., Suo, Z. & Evans, A. G. Thin film cracking and the roles of substrate and interface. *Int. J. Solids Struct.* **29,** 2639–2648 (1992).
12. Ball, P. *Nature's Patterns: a Tapestry in Three Parts* (Oxford Univ. Press, 2009).
13. Marder, M. & Fineberg, J. How things break. *Phys. Today* **49,** 24–29 (1996).
14. Bouchbinder, E., Fineberg, J. & Marder, M. Dynamics of simple cracks. *Annu. Rev. Cond. Matter Phys.* **1,** 371–395 (2010).
15. Sharon, E., Gross, S. P. & Fineberg, J. Local crack branching as a mechanism for instability in dynamic fracture. *Phys. Rev. Lett.* **74,** 5096–5099 (1995).
16. Yuse, A. & Sano, M. Instabilities of quasi-static crack patterns in quenched glass plates. *Physica D* **108,** 365–378 (1997).
17. Kobeda, E. & Irene, E. A. Intrinsic $SiO_2$ film stress measurements on thermally oxidized Si. *J. Vac. Sci. Technol. B* **5,** 15–19 (1987).
18. Cotterell, B. & Rice, J. R. Slightly curved or kinked cracks. *Int. J. Fract.* **16,** 155–169 (1980).
19. He, M.-Y. & Hutchison, J. W. Kinking of a crack out of an interface. *J. Appl. Mech.* **56,** 270–278 (1989).
20. Choi, S. T. & Earmme, Y. Y. Elastic study on singularities interacting with interfaces using alternating technique: Part I. Anisotropic trimaterial. *Int. J. Solids Struct.* **39,** 943–957 (2002).
21. Choi, S. T. & Earmme, Y. Y. Elastic study on singularities interacting with interfaces using alternating technique: Part II. Isotropic trimaterial. *Int. J. Solids Struct.* **39,** 1199–1211 (2002).
22. Faber, K. T. & Evans, A. G. Crack deflection processes – I. Theory. *Acta Metall.* **31,** 565–576 (1983).
23. Green, D. J., Tandon, R. & Sglavo, V. M. Crack arrest and multiple cracking in glass through the use of designed residual stress profiles. *Science* **283,** 1295–1297 (1999).
24. Rao, M. P., Sánchez-Herencia, A. J., Beltz, G. E., McMeeking, R. M. & Lange, F. F. Laminar ceramics that exhibit a threshold strength. *Science* **286,** 102–105 (1999).
25. Clegg, W. J. Controlling cracks in ceramics. *Science* **286,** 1097–1099 (1999).
26. Son, Y. *et al.* Nanoscale electronics: digital fabrication by direct femtosecond laser processing of metal nanoparticles. *Adv. Mater.* **23,** 3176–3181 (2011).
27. Xia, Y. *et al.* One dimensional nanostructures: synthesis, characterization, and applications. *Adv. Mater.* **15,** 353–389 (2003).
28. Nam, S. W. *et al.* Sub-10-nm nanochannels by self-sealing and self-limiting atomic layer deposition. *Nano Lett.* **10,** 3324–3329 (2010).
29. Marder, M. Cracks takes a new turn. *Nature* **362,** 295–296 (1993).
30. Buehler, M. J. & Gao, H. Dynamical fracture instabilities due to local hyperelasticity at crack tips. *Nature* **439,** 307–310 (2006).


**Supplementary Information** is linked to the online version of the paper at www.nature.com/nature.

**Acknowledgements** This research was supported by Creative Research Initiatives (Research Center of MEMS Space Telescope) of MEST/NRF. We thank Y.Y. Earmme at KAIST for discussions and J. Yeo, Y. D. Suh, S. Hong, P. Lee, Y. Rho and J.-A. Jeon for technical assistance with fabrications and experiments.

**Author Contributions** K.H.N. conceived the study, discovered the control of cracking using microfabrication, conducted experiments and theoretical study of the phenomena, and invented DISL. K.H.N. and I.H.P. designed mask patterns for photolithography and fabricated samples. S.H.K. did the post-processing and conducted experiments. K.H.N. and S.H.K. wrote the paper and discussed the results. All authors commented on the manuscript.

**Author Information** Reprints and permissions information is available at www.nature.com/reprints. The authors declare no competing financial interests. Readers are welcome to comment on the online version of this article at www.nature.com/nature. Correspondence and requests for materials should be addressed to K.H.N. (koonam@namk.org) or S.H.K. (maxko@kaist.ac.kr).